Original Paper

nephron
Physiology

Nephron Physiol 110
DOI: 10.1159/000XXXXXX

Received: April 10, 2008
Accepted: September 26, 2008
Published online: ■■■

Altered Renal Expression of Na^+ Transporters and ROMK in Protein-Deprived Rats

María Celeste Ruete[a] Liliana C. Carrizo[b] María Victoria Bocanegra[a]
Patricia G. Vallés[a, b]

[a]IMBECU-CONICET (Consejo Nacional de Investigaciones Científicas y Tecnológicas), [b]Área de Fisiopatología, Departamento de Patología, Facultad de Ciencias Médicas, Universidad Nacional de Cuyo, Mendoza, Argentina

Key Words
Sodium transporters · Hypokalemia · Low-protein diet

Abstract
Potassium depletion has been associated with altered sodium reabsorption in tubule segments. We studied if the altered abundance of Na^+ transporters and ROMK are associated with distal potassium secretion that contributes to the development of hypokalemia in protein-deprived rats. After weaning, Wistar rats were fed with a low-protein diet (8%, LP) for 14 days and then recovered with a normal-protein (NP) diet (24%, RP). An age-matched control group was fed with an NP diet (24%, NP). We showed hypokalemia, lower glomerular filtration rate and higher FEK^+ in the LP group. Immunoblotting revealed that the type 3 Na^+/H^+ exchanger in the cortex was decreased in the LP group. However, the type 2 Na^+-K^+-$2Cl^-$ cotransporter was increased in the outer stripe of the outer medulla in the LP group. The abundance of the aldosterone-regulated Na^+-Cl^- cotransporter (NCC) and epithelial Na^+ channel (ENaC) was higher in the LP group and was associated with higher plasma aldosterone level. ROMK protein levels were increased. Na^+/K^+-ATPase protein levels were the same in both groups. After the recovery period, the expression of Na^+ transporters and ROMK returned to control values. We conclude that increased expression of NCC, ENaC subunits, and ROMK contributed to distal potassium secretion leading to enhanced potassium excretion, which may explain the hypokalemia resulting from LP feeding. A role of aldosterone may be suggested.

Introduction

Clinical and experimental models of low-protein (LP) feeding have confirmed important alterations in renal hemodynamics, renal concentration capacity, and renal acid excretion [1]. Ichikawa et al. [2] showed reduced renal blood flow and glomerular filtration rate (GFR) as a result of increased renal vascular resistance in rats. The increased expression of renal renin mRNA, angiotensin I-converting enzyme mRNA, and AT_1 mRNA with reduced binding density on the AT_1 receptor in the renal cortex and outer medulla may ensure local angiotensin II generation, which in the presence of low renal cortical prostaglandin synthesis would contribute to the vasoconstriction in an LP diet [3–5].

This study was presented in an abstract form at the 14th Congress of the International Pediatric Nephrology Association, 31 August to 4 September, 2007, Budapest.

KARGER

Fax +41 61 306 12 34
E-Mail karger@karger.ch
www.karger.com

1660–2137/08/0000–0000$26.00/0

Accessible online at:
www.karger.com/nep

Dr. Patricia G. Vallés
Area de Fisiología Patológica, Departamento de Patología
Facultad de Ciencias Médicas, Universidad Nacional de Cuyo
Centro Universitario, 5500 Mendoza (Argentina)
Tel. +54 261 413 5000, Fax +54 261 428 7370, E-Mail pvalles@fcm.uncu.edu.ar

Injury events caused by an LP diet – an in vivo model of energy deprivation – include ATP depletion on epithelial cells from medullary duct segments [5, 6] and renal hemodynamic changes [4]. After administration of a 6% protein diet, in vivo microperfusion of the loop of Henle showed a high sodium concentration in early distal tubule fluid resulting from a reduced sodium net reabsorptive rate (J_{Na}) with decreased Na^+/K^+-ATPase activity in microdissected medullary TAL (mTAL) [6]. Recently, we provided evidence for the transient disruption of the Na^+/K^+-ATPase from its cellular localization in the cytoskeleton anchorage and migration to the apical membrane in the outer stripe of the outer medulla in the LP group [7]. Findings of altered plasma electrolytes in an LP diet include potassium depletion, a frequent electrolyte disturbance that contributes to the high morbidity and mortality in LP [8, 9].

The direction and magnitude of the potassium transport in the various nephron segments depend on the site-specific distribution of transporters in the membranes of tubule cells [10]. The correction of deviations from normal plasma K^+ levels and the maintenance of external K^+ balance depend on the intrinsic ability of distal nephron segments to either secrete or reabsorb K^+. Net K^+ secretion occurs mainly in principal cells, while K^+ absorption takes place in intercalated cells [11]. The small conductance channels are the most abundant K^+ channel type in the apical membrane of the mammalian cortical collecting ducts (CCDs) and connecting tubule [12]. These channels are encoded by the ROMK gene [13, 14], which was confirmed by the absence of the channels in a ROMK knockout mouse strain [15]. ROMK are the predominant route for K^+ secretion by the distal nephron. Enhanced delivery of fluid and Na^+ to the distal tubule is one of the most powerful and frequently activated mechanisms of distal tubule K^+ secretion [16].

Adjustments of the amount of sodium available in the distal tubule lumen and of the Na^+ excretion occur, in part, through adaptive changes in the abundance of apical Na^+ transporter proteins expressed in the various renal tubule segments [17, 18].

The major apical Na^+ transporters that notably contribute to this regulation are the type 3 Na^+/H^+ exchanger (NHE3) in the proximal tubule (PT), the bumetanide-sensitive type 2 Na^+-K^+-$2Cl^-$ cotransporter (NKCC-2) in the thick ascending limb of Henle, the thiazide-sensitive Na^+-Cl^- cotransporter (NCC) in the distal convoluted tubule (DCT), and the amiloride-sensitive epithelial Na^+ channel (ENaC) in the connecting tubules and collecting ducts [19, 20].

The strong dependence of potassium secretion on distal sodium supply explains that an increase in the delivery of sodium-containing fluid to the distal tubule increases potassium secretion [21]. In addition, plasma aldosterone levels, which are critically involved in controlling sodium balance, are involved in the regulation of potassium transport [22].

Our aim was to demonstrate the altered expression of the major sodium transporters and potassium channel ROMK in the rat kidney during an LP diet. We also examined if the changes in the protein levels of these transporters contribute to increased potassium secretion leading to excretion. This excretion might explain the hypokalemia resulting from an LP diet.

Material and Methods

Experimental Animals and Protocol

Female Wistar rats weighing 60–70 g were used in all the experiments. During a preliminary study, we estimated that the minimum amount of food ingested by the rats in the metabolic cages was 10 g/day. Rats had unlimited access to water and food consumption. The body weight of each animal was measured daily.

The animals were divided into three dietary groups. The normal protein (NP) group (n = 12) received an isocaloric 24% protein diet during 14 days (NP_{14}; age-matched control group of the LP group) or during 30 days (NP_{30}; age-matched control group of the recovery protein, RP, group). This group's diet was composed of casein (24%), cornstarch (36%), sucrose (21.3%). The LP group (n = 12) received an isocaloric 8% protein diet for 14 days. This group's diet was composed of casein (8%), cornstarch (48.45%), and sucrose (24.3%). Both diets contained cellulose fiber (10%), choline (0.2%), mineral mix (2%), vitamin mix (0.5%), corn-oil (6%), 0.069 mEq of Na^+ per gram, and 0.16 mEq of K^+ per gram. The RP group (n = 12) received a readministration of 24% protein for 14 days after being fed with 8% LP diet for 14 days.

Blood pressure was measured by tail-cuff plethysmography (Grass model 7B Poligraph, Grass Instruments, Quincy, Mass., USA) in the rats on days 14 and 30 after the initiation of the experimental protocol.

Animals were deeply anaesthetized with sodium pentobarbital (60 mg/kg intraperitoneal).

Animal experimental procedures in this study have been approved by the Laboratory Animal Ethical Committee of the School of Medicine, Cuyo University, Mendoza (32/95CD), and were conducted in accordance with guidelines of the Ethical Committee of Clinical Experimentation of Argentina.

Urinary and Plasma Measurements

Three days before the 24-hour urine collection, rats from each group were placed in metabolic cages for acclimatization to the cages. After 14 days of dietary pretreatment, urine was collected during a 24-hour period. Under anesthesia, blood was collected into a heparinized tube to determine creatinine, osmolarity, and

sodium and potassium concentration. Aliquots of each urine sample were promptly frozen at –20°C. Arterial blood samples were also obtained from animals in each group and were collected from the aorta immediately after anesthesia. We measured the urine and plasma electrolytes using an ion-selective electrode (Beckman Electrolyte 2 analyzer), creatinine using a Hitachi 912-Roche auto-analyzer. Plasma aldosterone concentrations were determined with a solid-phase ^{125}I radioimmnunoasay kit (Coat-A-Count Aldosterone; Diagnostic Products Corporation, Los Angeles, Calif., USA).

Tissue Preparation for Western Blot

To rinse all the blood, we perfused the kidneys through the abdominal aorta with ice-cold phosphate-buffered saline (PBS) solution. From the samples in all groups, the cortex and the outer stripe of the outer medulla were isolated and homogenized in chilled extraction buffer containing 20 mM Tris-HCl, 250 mM sucrose, 5 mM EDTA, 0.5 mM PMSF, 10 μg/ml leupeptin, and 5 μg/ml trypsin inhibitor (pH 7.4). We used a Duonce-style tissue homogenizer to obtain the homogenate. The homogenate was then centrifuged at 6,000 *g* for 15 min at 4°C. The pellet was discarded, and the supernatant was recentrifuged at 45,800 *g* for 45 min at 4°C. The new pellet obtained was resuspended in 100 μl of extraction buffer. Aliquots of each condition were stored at –70°C.

Primary Antibodies

For semiquantitative immunoblotting and immunofluorescence, we used the following polyclonal antibodies: NHE3 (Chemicon), dilution 1:2,500; NKCC-2 (Chemicon), 1:2,000; ROMK (Chemicon), 1:2,000; Na^+/K^+ATPase (Upstate), 1:1,000; NCC (Chemicon), 1:2,000; α-ENaC (Chemicon), 1:2,500; β-ENaC (Chemicon), 1:2,500, and γ-ENaC (Chemicon), 1:2,500.

Protein Determination and Western Blot Analysis

We quantified the protein concentration from the cortex, cortex/outer stripe of the outer medulla, or the outer stripe of the outer medulla by Lowry assay. We used BSA 10 mg/ml as a standard. Protein samples were prepared in SDS sample buffer (31.25 mM Tris-HCl pH 6.8, 10% glycerol, 0.0025% bromophenol blue, and 10 mM DTT, 1% SDS). We electrophoresed 20 μg of proteins in 0.1% SDS and 8% polyacrylamide gel with 4% stacking gel. Two identical gels were run in parallel. One gel was subjected to Coomassie blue staining to assure identical loading. The other gel was subjected to immunoblotting. Proteins were electrophoretically transferred from gels to nitrocellulose membranes. Nonspecific reactivity was blocked by incubation for 1 h at room temperature with 5% nonfat dry milk dissolved in PBS (pH 7.6, 0.1% Tween 20). Blots were incubated overnight with affinity-purified primary antibodies at 4°C (NHE3, α-ENaC, β-ENaC, γ-ENaC, NCC, NKCC-2, ROMK, and Na^+/K^+-ATPase). The labeling was visualized with secondary biotinylated antibodies and then with horseradish peroxidase-conjugated streptavidin (DAKO). The signal was detected with an enhanced chemiluminescence system and with X-ray film (Amersham).

Densitometric analysis was performed with the US National Institutes of Health Image 1.66 software (National Institutes of Health, Bethesda, Md., USA). In order to quantify the blots (Western blot analysis) by densitometry, for each antibody, the amount of total protein loaded was the one that lies on the part of the curve where the relationship between amount loaded and pixel density was linear. For most of the antibodies, the amount of loaded protein was 20 μg. To facilitate comparisons, the magnitude of the immunosignal was normalized to control by defining the mean for the control group as 100%.

Preparation of Tissue for Immunofluorescence

To rinse all the blood, we perfused the kidneys through the abdominal aorta with ice-cold PBS solution. Then the kidneys were fixed by retrogade perfusion with 40 ml of 4% paraformaldehyde in 9.4 mM $Na_2B_4O_7$, 0.34 mM Na_2SO_3, and 0.16 M H_3BO_3 (pH 7.4). The kidneys were removed and placed in paraformaldehyde for 4 h at room temperature and overnight at 4°C. Fixed tissues were cryoprotected in 0.9 M sucrose, washed in PBS several times, frozen in isopentane, and stored at –70°C.

Indirect Immunofluorescence

Five-micrometer-thick cryosections were placed on slides pretreated with 3-aminopropyltriethoxysilane. Sections were incubated in 50 mM $ClNH_4$ for 2 h. Nonspecific staining was blocked with 1% BSA in PBS containing 1% SDS and 1% Triton X-100 (PBS/BSA/Triton) for 1 h at room temperature. After a rinse with PBS for 5 min, sections were incubated overnight at 4°C with anti-NHE3 polyclonal antibody diluted 1:100 in PBS/BSA/Triton or in anti-ROMK polyclonal antibody diluted 1:100 in PBS/BSA/Triton. Sections were then rinsed with PBS for 10 min and with PBS high-salt (2.7% NaCl) for 5 min and covered for 1 h at room temperature with secondary antibody 1:100. After a rinse with PBS, sections were incubated for 1 h with streptavidin-FITC diluted 1:100 in PBS/BSA/Triton. Finally, the sections were rinsed with PBS high-salt and mounted into PBS:glycerol (1:1). We used epifluorescence microscopy to examine the slides.

Microdissection of Tubule Segments

The right kidneys were cut along the corticopapillary axis. We placed 1-mm-thick slices into the dissection solution at 4°C containing (in mM) 100 NaCl, 3.7 Cl_2Mg, 2 $CaCl_2$, 66.7 NH_4Cl, 50 imidazole, and 5.5 glucose, without collagenase, and immediately microdissected by hand with the aid of fine stainless steel needles under a stereomicroscope (×10–40). The outer medullary proximal straight tubules (S3) were dissected by locating the beginning of a descending thin limb of Henle in the outer medulla and dissecting towards the cortex. CCDs measuring 0.5–1 mm in length were dissected from the medullary ray distal to the junction of two renal tubules. From the outer stripe of the outer medulla, OMCD segments were dissected deep to the corticomedullary junction [23]. Between 8 and 10 S3, CCD and OMCD segments were dissected from each animal. The length of each tubule was measured under the stereomicroscope with an eyepiece micrometer.

Assay for Na^+/K^+-ATPase Activity

The Na^+K^+-ATPase activity was measured in the presence of ouabain by the malachite-green colorimetric method, as described previously [24]. The total ATPase activity was measured by the rate of inorganic phosphate (P_i). The microdissected tubule segments were permeabilized in 4 μl permeabilization buffer (Imidazole 100 mM, BSA 1 mg/ml), frozen for 15 min, thawed at room temperature, and permeabilized again. Then the S3, CCD and OMCDs were incubated for 15 min at 37°C in the presence of 10 μl ATP 1 mM with ouabain 1 mM to determine the Mg^{2+}-

Table 1. Body weight, kidney weight, and blood pressure

	NP_{14}	LP	NP_{30}	RP
Initial body weight, g	55 ± 2.3	51 ± 3.4	52 ± 3.5	54 ± 2.9
Final body weight, g	121.3 ± 3.6	65.9 ± 2.2*	152.1 ± 5.57	147.8 ± 4.98
Kidney weight, g	0.69 ± 0.04	0.33 ± 0.03*	0.72 ± 0.07	0.69 ± 0.09
Initial blood pressure, mm Hg	104.3 ± 2.6	105.2 ± 2.9	103.2 ± 3.1	106 ± 3.11
Final blood pressure, mm Hg	106 ± 2.10	107 ± 1.69	116.3 ± 5.8	117.5 ± 5.11

Data represent the mean ± SEM (n = 12); * $p < 0.05$.

Table 2. Functional data

	$NP_{14 \text{ and } 30}$ (n = 12)	LP (n = 12)	RP (n = 12)
Cl_{Cr}, ml/min·100 g	1.59 ± 0.21	0.96 ± 0.10*	1.46 ± 0.19
P_{K+}, mM	4.32 ± 0.23	3.05 ± 0.1*	4.46 ± 0.15
P_{Na+}, mM	142 ± 3	140 ± 5	141 ± 3
FE_{K+}, %	29.9 ± 0.3	42.2 ± 0.5*	26.3 ± 0.2
FE_{Na+}, %	1.2 ± 0.05	1.4 ± 0.06	1.2 ± 0.16
UV, µl/min·kg	16.47 ± 0.27	19.23 ± 0.15*	15.23 ± 0.1
$P_{aldosterone}$, pg/ml	202 ± 12	285.8 ± 37*	147 ± 47
P_{urea}, mM	7.8 ± 1.9	2.31 ± 0.9*	6.66 ± 0.8
U_{urea}, mM	406 ± 45	233.9 ± 36*	446.2 ± 52

Cl_{Cr} = Creatinine clearance; P_{K+} = plasma potassium; P_{Na+} = plasma sodium; FE_{K+} = potassium fractional excretion; FE_{Na+} = sodium fractional excretion; UV = urinary volume; $P_{aldosterone}$ = plasma aldosterone; P_{urea} = plasma urea; U_{urea} = urine urea. Data represent the mean ± SEM; * $p < 0.05$ vs. $NP_{14 \text{ and } 30}$.

ATPase activity, or without ouabain to determine total ATPase activity. Na^+/K^+-ATPase activity was defined as the difference between the total and the Mg^{2+}-ATPase activities. For each animal, the Na^+/K^+-ATPase activity was made in triplicate samples for different experimental conditions. The mean value was considered as a single point. The final result represents the mean ± SEM of 6 animals. In each experiment, blanks were also run in triplicate to measure the nonenzymatic hydrolysis of P_i. The Na^+/K^+-ATPase activity was expressed as pmol of inorganic phosphate per minute per millimeter of tubule length.

Statistical Analysis

The results were assessed by one-way analysis of variance to compare the three groups. Significance of differences was estimated by the Bonferroni test. A $p < 0.05$ was considered significant. Values were expressed as means ± SEM.

Results

For the 14-day period of pair feeding, average daily food intakes were 14.32 ± 0.42 g/100 g body weight in the NP group and 14.71 ± 0.37 g/100 g body weight in the LP group. The body weight and the kidney weight in the LP group were significant lower than in the NP group (table 1; $p < 0.05$ for both). No differences were observed in the blood pressure (mm Hg) among groups (table 1). The levels of plasma urea nitrogen in the LP group were significantly decreased (table 2; $p < 0.05$, n = 12). Urine urea nitrogen was also lower in the LP group than in the NP group (table 2; $p < 0.05$, n = 12). The creatinine clearance was lower in the LP group than in the NP group (table 2; $p < 0.05$, n = 12), a result that is consistent with previous studies using this experimental model.

Rats in the LP group developed hypokalemia, and had lower plasma potassium levels (table 2; $p < 0.05$, n = 12). The fractional excretion of potassium was higher in the LP group than in the NP group (table 2; $p < 0.05$, n = 12). Along with this, the rats in the LP group had greater water excretion than rats in the NP group. Urinary output was significantly higher in the LP group compared with the NP group (table 2; $p < 0.05$, n = 12). The higher urinary output was also associated with lower urinary os-

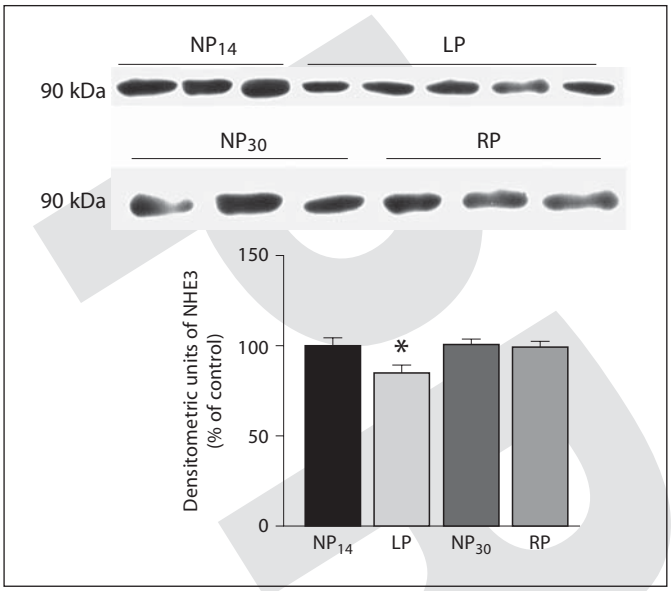

Fig. 1. Semiquantitative immunoblotting of membrane fractions of the cortex. Immunoblots reacted with anti-NHE3 antibody revealed a single ~90-kDa band. The intensity of the bands was quantified by densitometry and was expressed as arbitrary units. Densitometric analysis revealed a decrease in NHE3 abundance in the LP group compared with the NP group (* $p < 0.05$). No significant differences were observed between the RP group and the NP group. Data represent the mean ± SEM (n = 12).

molarity (923 ± 110 vs. 1,196 ± 61 mosm/kg H_2O, $p < 0.05$, n = 12). In contrast to the marked alteration in water and potassium balance in the LP group, plasma sodium levels and fractional excretion of sodium were unchanged in both groups of rats (table 2). The LP group had higher plasma aldosterone levels than the NP group (table 2; $p < 0.05$, n = 12).

Reduction in NHE3 Abundance in the Kidney Cortex of Rats Fed an LP Diet

In renal PTs, apical Na^+/H^+ exchange mediates most of the transcellular NaCl transport and two thirds of the transcellular $NaHCO_3^-$ [25], and NHE3 plays a major role in this process [26]. The anti-NHE3 antibody recognized a ~90-kDa band in the membrane preparations from the kidney cortex. No other bands were identified by the antibody. Densitometric analysis of membrane fractions from the LP group revealed a significant decrease in NHE3 levels compared with the NP group (85 ± 5 vs. 100 ± 2%, $p < 0.05$, n = 12; fig. 1). The results indicated the recovery of NHE3 protein levels to control values during the readministration of 24% protein diet (fig. 1). Consistent with these results, immunofluorescence analysis confirmed that the expression of NHE3 in the LP group was less than in the NP group. The anti-NHE3 antibody strongly labeled the apical domains of the PT, whereas basolateral plasma membranes were unlabelled in kidney sections of the NP group. In contrast, NHE3 labeling was lower in the apical membranes of the PTs from the cortex (fig. 2) and the PT from the outer stripe of the outer medulla (OSOM; not shown) in kidney sections of the LP

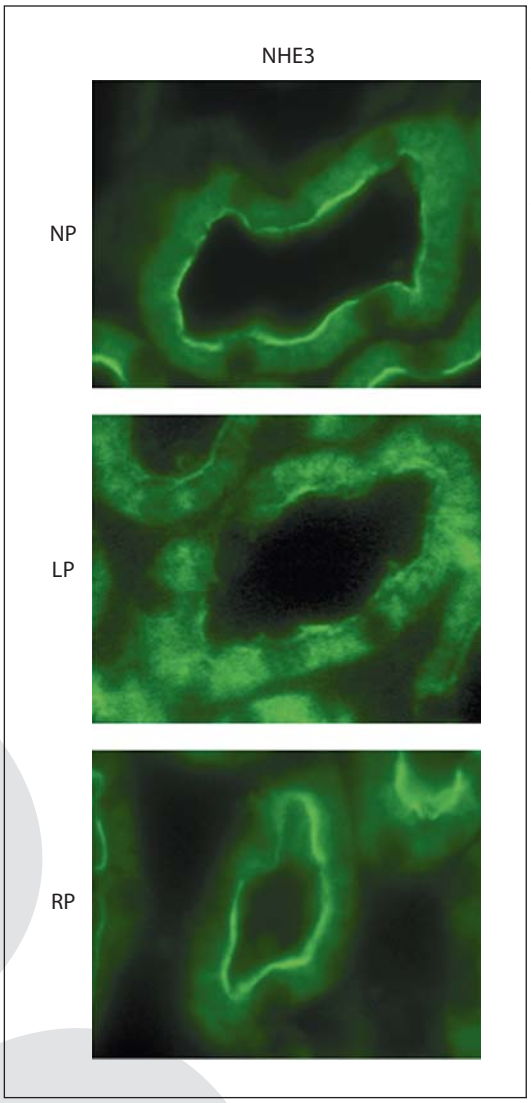

Color version available online

Fig. 2. Effect of LP diet on NHE3 immunofluorescence. Frozen tissues were fixed and stained with an anti-NHE3 antibody. These data revealed that NHE3 showed a higher signal in the apical domains of the PT in the LP group than in the NP group. In the RP group, the signal showed no significant differences compared with the NP group. Magnification ×600.

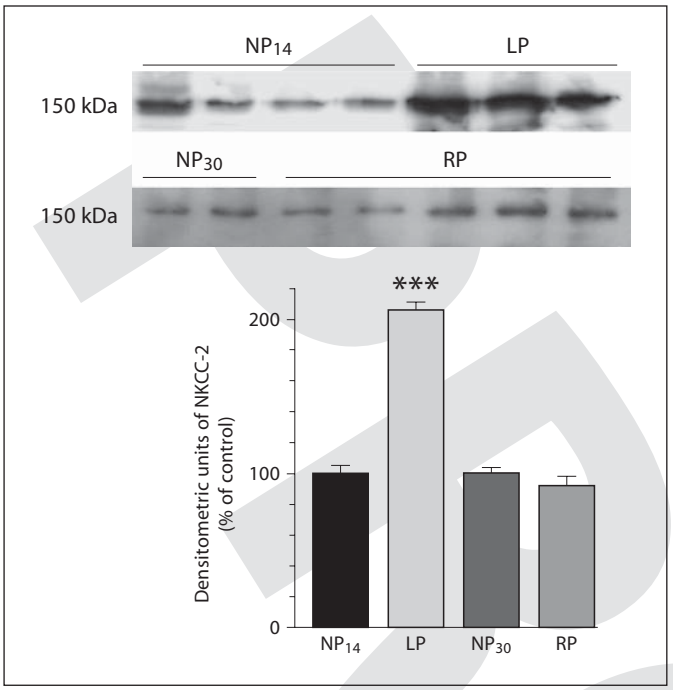

Fig. 3. Semiquantitative immunoblotting of membrane fractions of the outer stripe of the outer medulla. Immunoblots reacted with anti-NKCC-2 antibody revealed a single ~150-kDa band. The intensity of the bands was quantified by densitometry and was expressed as arbitrary units. Densitometric analysis revealed higher NKCC-2 abundance in the LP group than in the NP group (*** $p < 0.001$). No significant differences were observed between the RP group and the NP group. Data represent the mean ± SEM (n = 12).

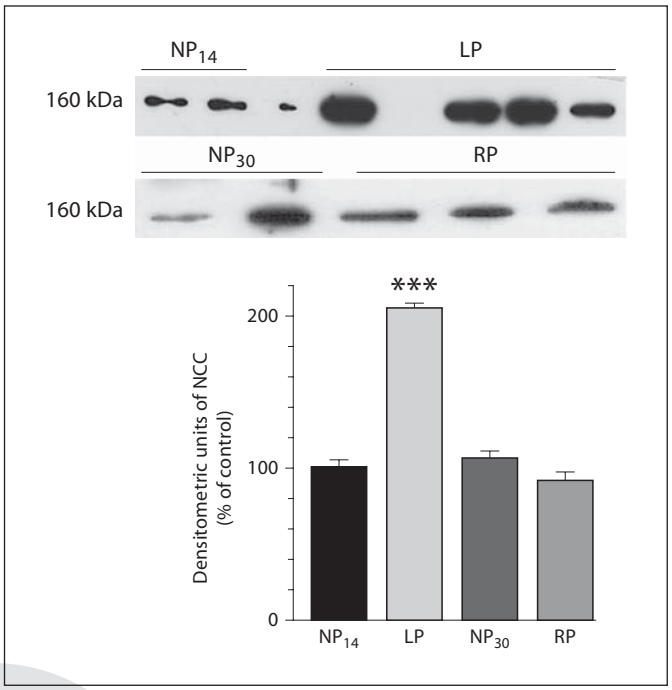

Fig. 4. Semiquantitative immunoblotting of membrane fractions of the cortex. Immunoblots reacted with anti-NCC antibody revealed a single ~160-kDa band. The intensity of the bands was quantified by densitometry and was expressed as arbitrary units. Densitometric analysis revealed higher NCC abundance in the LP group than in the NP group (*** $p < 0.001$). No significant differences were observed between the RP group and the NP group. Data represent the mean ± SEM (n = 12).

group than the NP group. After the recovery period, the NHE3 immunoreaction in the apical domain of epithelial cells from PT in the LP group was similar to the control.

Kidney Levels of Two Major Absorptive Na^+-K^+-Cl^- Cotransporters NKCC-2 in the TAL and Na^+-K^+ Cotransporter NCC in the DCT Are Higher in the LP Group than in the NP Group

NKCC-2 is the major transporter for apical sodium reabsorption in the mTAL and cortical TAL (cTAL). Western blot analysis showed that NKCC-2 antibody recognized a broad band centered at ~150 kDa (fig. 3) as reported by Ecelbarger et al. [27]. No other bands were identified by the antibody. In contrast to the significantly lower kidney cortex levels of NHE3 in the LP group, we found higher levels of NKCC-2 in OSOM in the LP group than in the NP group (190 ± 6 vs. 100 ± 4%, $p < 0.001$, n = 12; fig. 3). At the luminal membrane of the DCT, the apical thiazide-sensitive NCC is the major pathway for salt reabsorption. In the cortex, the anti-NCC antibody recognized a protein with a molecular mass centered at ~160 kDa. Densitometric analysis showed that NCC abundance was significantly higher in the LP group than in the NP group (204 ± 2 vs. 100 ± 4%, $p < 0.001$, n = 12; fig. 4). After the recovery period, the abundance of NKCC-2 and NCC returned to control levels.

Increased Protein Expression of ENaC Subunits

We studied the abundance of ENaC subunits in the cortex/OSOM of kidneys and found that α-ENaC, β-ENaC, and γ-ENaC were increased in the LP group. No other bands were identified by the antibody. We found significantly more α-ENaC in the kidney cortex/OSOM in the LP group than in the NP group (206.3 ± 4 vs. 100 ± 3%, $p < 0.001$, n = 12; fig. 5a). In addition, the protein abundance of the β- and γ-subunits of ENaC in the kidney cortex/OSOM of the LP group was also higher. Pro-

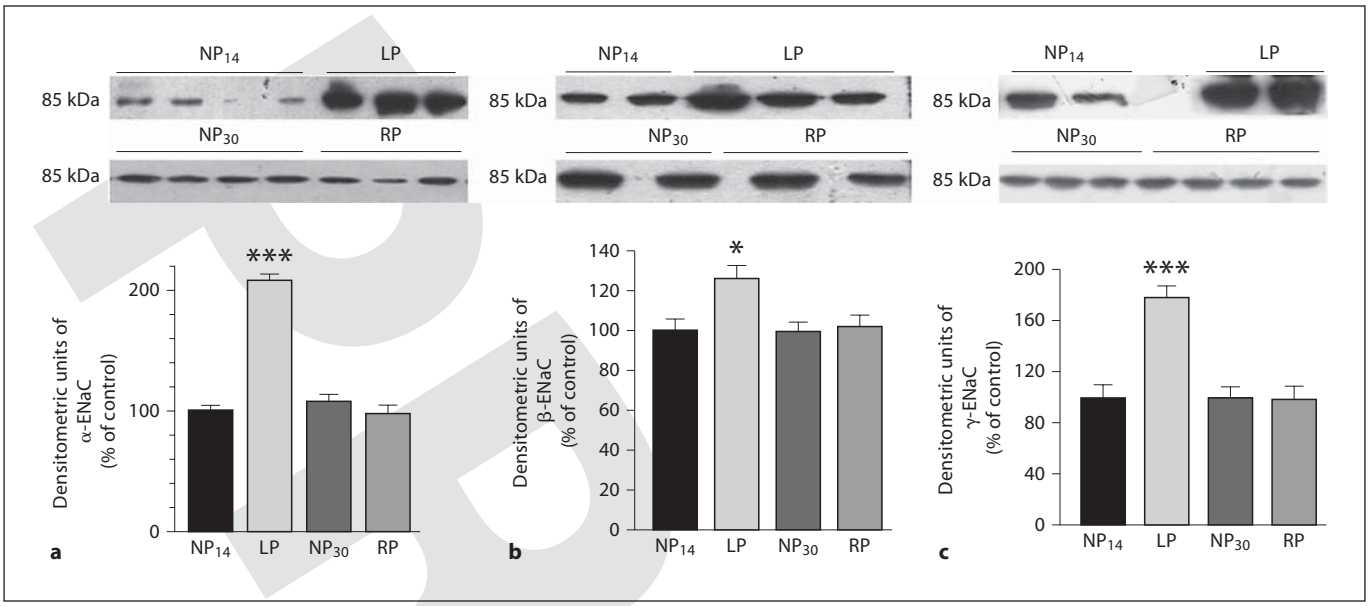

Fig. 5. Semiquantitative immunoblotting of membrane fractions of the cortex/outer stripe of the outer medulla. Immunoblots reacted with anti-α-ENaC antibody (**a**), anti-β-ENaC antibody (**b**), and anti-γ-ENaC antibody (**c**), and each revealed a single ~85-kDa band. The intensity of the bands was quantified by densitometry and was expressed as arbitrary units. Densitometric analysis revealed a higher abundance of the three subunits of ENaC in the LP than in the NP group. No significant differences were observed between the RP group and the NP group. Data represent the mean ± SEM (n = 12); *** $p < 0.001$, * $p < 0.05$.

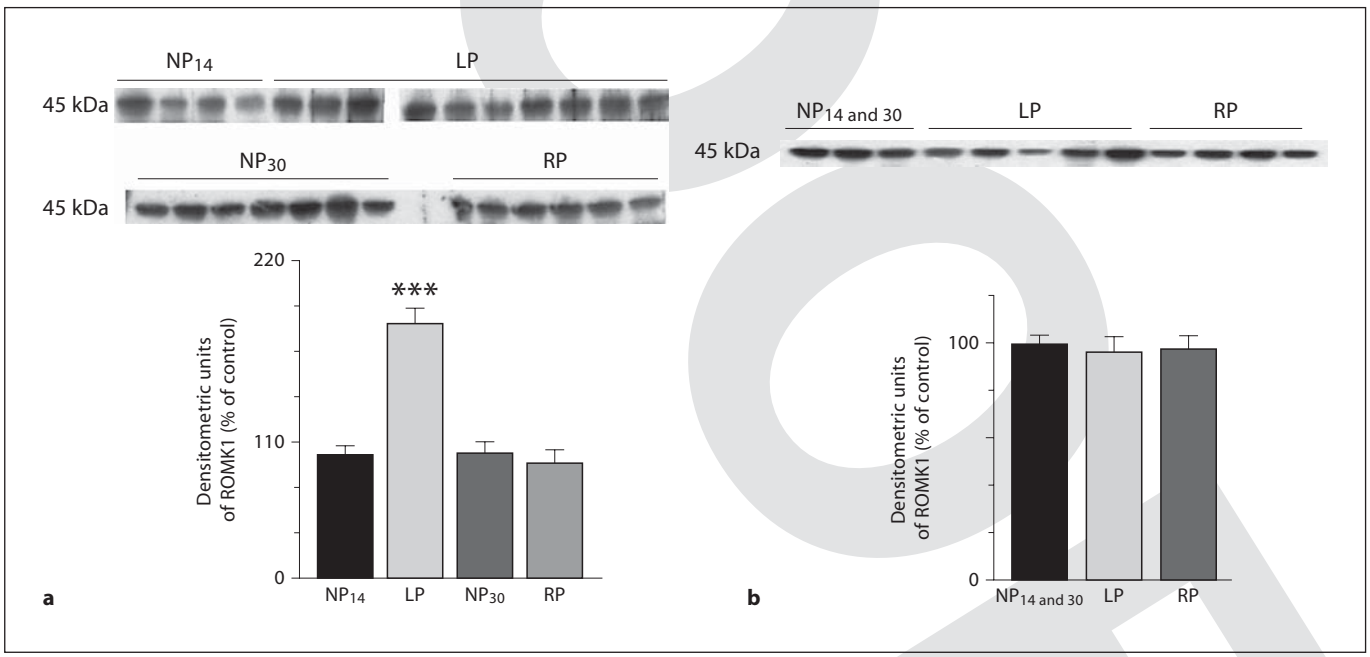

Fig. 6. Semiquantitative immunoblotting of membrane fractions of the cortex and outer medulla. Immunoblots reacted with anti-ROMK1 antibody revealed a single ~45-kDa band. The intensity of the bands was quantified by densitometry and was expressed as arbitrary units. **a** Densitometric analysis revealed higher abundance in ROMK1 in the LP group than in the NP group (*** $p < 0.001$) in the cortex. **b** No significant differences were observed between the LP group and the NP group in the outer medulla and between the RP group and the NP group. Data represent the mean ± SEM (n = 12).

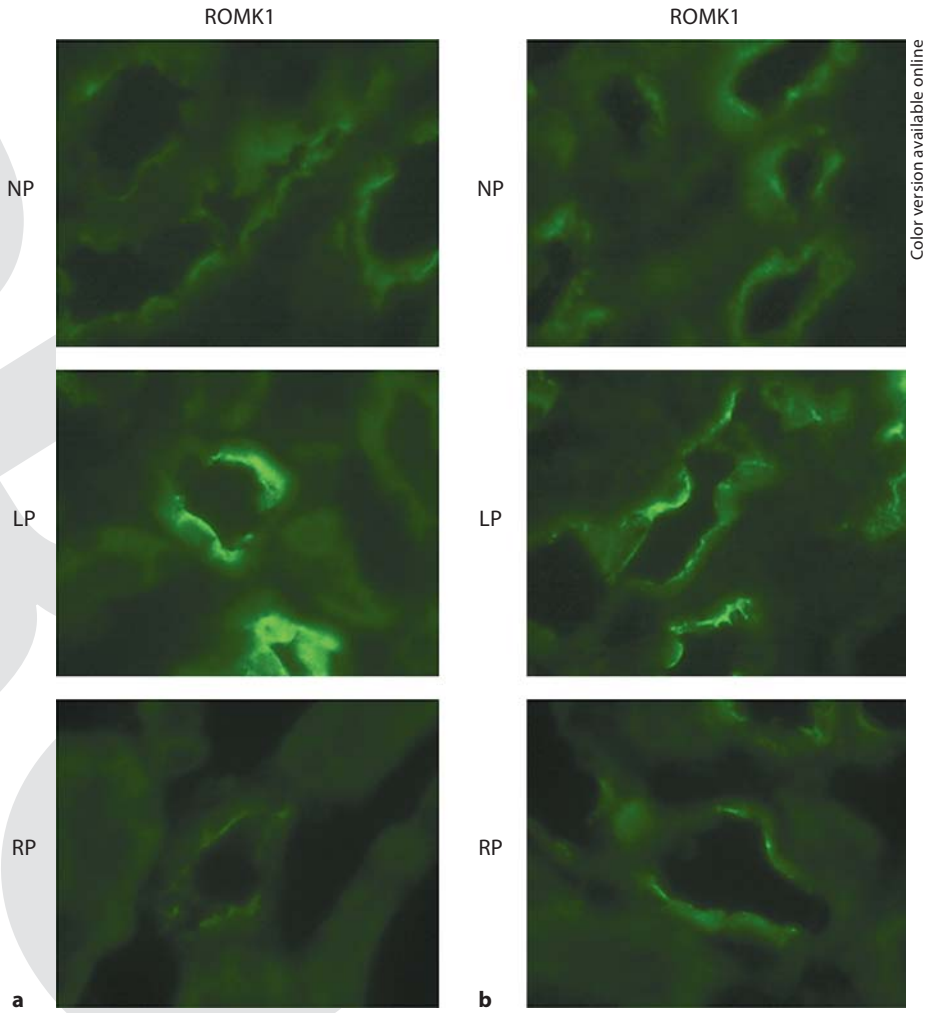

Fig. 7. Effect of LP diet on ROMK1 immunofluorescence in the cortex and the outer medulla. Frozen tissues were fixed and stained with an anti-ROMK1 antibody. These data revealed that ROMK1 showed a higher signal in CCD segments in the cortex (**a**) and in both OMCD and mTAL segments in the outer medulla (**b**) from the LP group. In the RP group, the ROMK1 signal showed no significant differences compared with the NP group. Magnification ×600.

tein levels of β-ENaC (126 ± 6 vs. 100 ± 5%; n = 12, $p < 0.05$; fig. 5b) and γ-ENaC (178.35 ± 3.58 vs. 100 ± 4.3%, $p < 0.001$, n = 12; fig. 5c) were higher in the LP group compared with the NP group.

ROMK Protein Expression

The electrical driving force for apical Na^+ entry through ENaC is maintained by the K^+ channel ROMK. This channel is considered the most important to serve this function [28].

Because we found increased protein levels of the three ENaC subunits in cortex/OSOM membrane fractions in the LP group, we assessed if the ROMK protein was upregulated in the cortex.

Antibody generated to sequences of ROMK shared by all isoforms has demonstrated an apical pattern of channel protein expression, consistent with the ROMK channel providing a K^+ secretory pathway in renal epithelia [29]. The anti-ROMK antibody detected a band of ~45 kDa. No other bands were identified by the antibody. Densitometric analysis revealed that the protein abundance of ROMK was markedly higher in the cortex of the LP group than in the cortex of the NP group (204.4 ± 9.7 vs. 100 ± 5.7%, $p < 0.001$, n = 12; fig. 6a), while the abundance of ROMK in OSOM was the same in the two groups (fig. 6b). After the recovery period, the abundance of the ROMK in the cortex and the OSOM kidney membrane fractions was similar to the control.

Consistent with these findings, immunofluorescence analysis revealed higher ROMK labeling in the apical plasma membrane domains of CCD in the LP group than in the NP group (fig. 7a). The ROMK labeling at CCD in both the NP and RP groups was weak. We found a higher apical ROMK staining in *c*TAL cells in the LP group

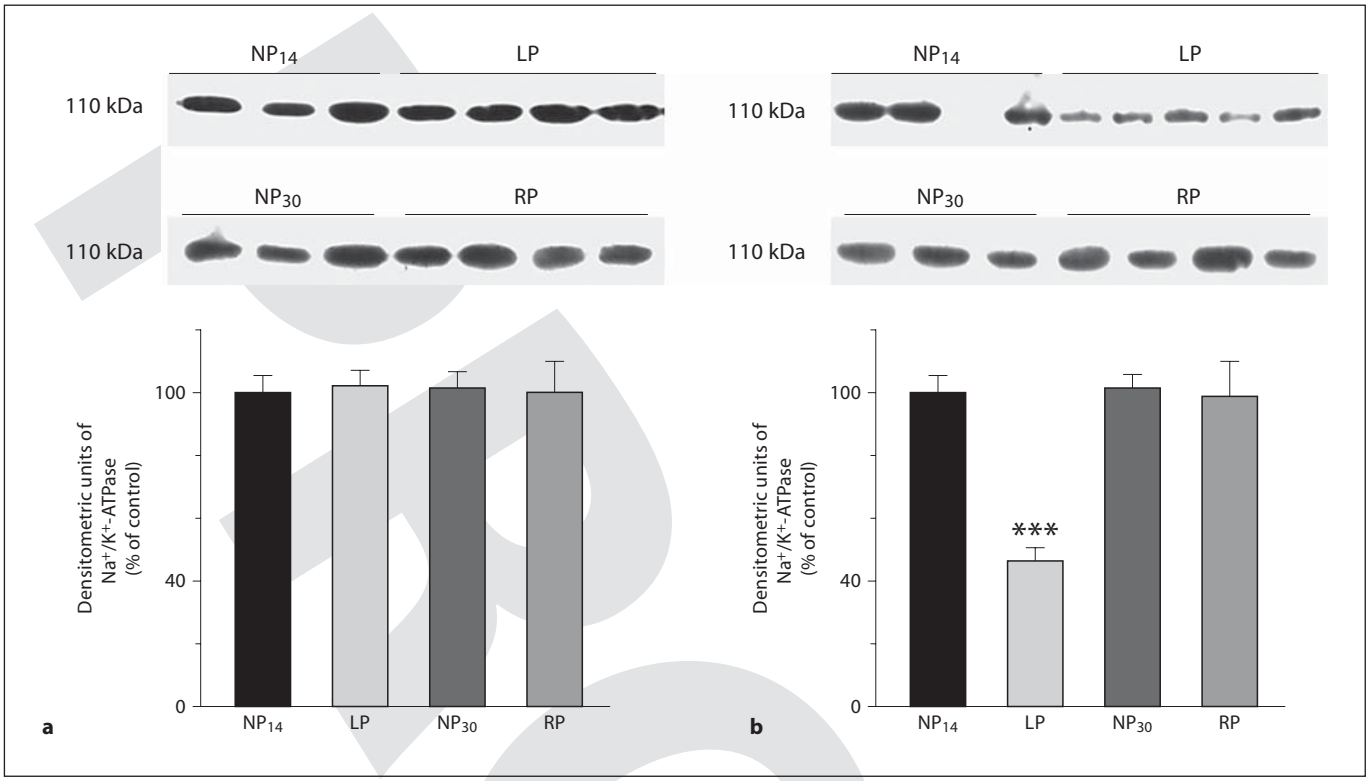

Fig. 8. Semiquantitative immunoblotting of membrane fractions of the cortex and outer medulla. Immunoblots reacted with anti-Na^+/K^+-ATPase antibody revealed a single ~110-kDa band. The intensity of the bands was quantified by densitometry and was expressed as arbitrary units. **a** No significant differences were observed between the LP group and the NP group in the cortex. **b** Densitometric analysis revealed higher abundance in Na^+/K^+-ATPase in the outer stripe of the outer medulla in the LP group than in the NP group (*** $p < 0.001$). No significant differences were observed between the RP group and the NP group. Data represent the mean ± SEM (n = 12).

than in the NP group (tubule cross sections positive for ROMK are not shown). We observed increased ROMK immunoreactivity at the apical domain of OMCDs and mTAL in the LP group (fig. 7b).

Effect of an LP Diet on Na^+/K^+-ATPase Expression and on the Activity of Microdissected CCDs

The renal tubule is rich in Na^+/K^+-ATPase, an important transport protein capable of coupling hydrolysis of ATP to the active translocation of sodium and potassium across the cell membrane and secondary active transport of other solutes.

Whereas the apical Na^+ transporters vary among the tubule segments, the basolateral Na^+/K^+-ATPase is common to each segment [30]. The α_1-isoform antibody recognized a band migrating at ~110 kDa. Semiquantitative immunoblotting of the α-subunit of the Na^+/K^+-ATPase showed that the protein abundance of the kidney cortex of the LP group and the NP group was the same (fig. 8a). However, the Na^+/K^+-ATPase α_1-subunit protein levels were lower in the kidney OSOM of the LP group than those of the NP group (46.8 ± 3.83 vs. 100 ± 5.1%, $p < 0.001$, n = 12; fig. 8b).

The immunofluorescence of Na^+/K^+-ATPase in the OSOM kidney sections showed less staining on the basolateral tubule membrane in the LP group than in the NP group (fig. 9).

We also analyzed the Na^+/K^+-ATPase activity (expressed as pmol/mm/min) in microdissected S3 PT, CCD and OMCDs. The Na^+/K^+-ATPase activity was significantly lower in the S3 PT and OMCD of the LP group than in that of the NP group (S3: 0.65 ± 0.10 vs. 0.05 ± 0.07, $p < 0.001$; OMCD: 2.4 ± 0.25 vs. 6.6 ± 0.42, $p < 0.001$, n = 8). However, there were no significant differences in the CCD Na^+/K^+-ATPase activity between the LP group and the NP group (10.36 ± 0.45 vs. 11.58 ± 0.32, $p > 0.05$, n = 8).

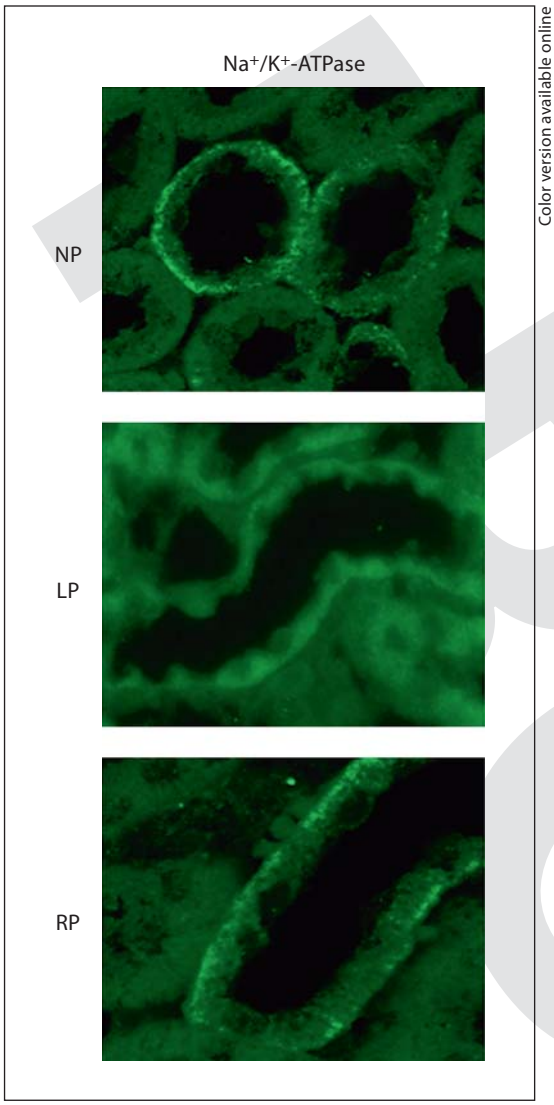

Fig. 9. Effect of LP diet on Na^+/K^+-ATPase immunofluorescence in the outer medulla. Frozen tissues were fixed and stained with an anti-Na^+/K^+-ATPase antibody. The Na^+/K^+-ATPase signal at the basolateral domain of outer medullary collecting ducts was lower for the LP group than for the NP group in the outer medulla. Na^+/K^+-ATPase immunoreaction showed no differences between the NP group and the RP group. Magnification ×600.

Discussion

We demonstrated that the expression of several major renal sodium transporters (NKCC-2, NCC, and ENaC subunits) and the potassium channel ROMK were significantly upregulated after the rats had been given the LP diet. These results were associated with enhanced potassium secretion, which contributed to hypokalemia. In contrast, the protein expression of NHE3 was downregulated in the PTs and the cTAL of the rat kidney.

Specifically, the increased expression of NCC, α-ENaC subunits, and ROMK indicates that these transporters contribute to Na^+ reabsorption and to potassium secretion associated with higher K^+ excretion at distal segments. We found higher plasma aldosterone levels in the LP group. The readministration of 24% protein in the diet recovered protein levels of sodium transporters and potassium channels to control values.

Reduced Abundance of NHE3 in the PTs and Increased Abundance of NKCC-2 in TALs in the LP Group

Injury events caused by an LP diet, an in vivo model of energy deprivation, include ATP depletion on epithelial cells from duct segments [7]. Disruption of PT function, which ultimately results in increased distal sodium and fluid delivery, is associated with renal hemodynamic changes including a decrease in the GFR and renal plasma flow. Moreover, micropuncture studies in LP diets have revealed decreased single-nephron GFR as a result of higher afferent and efferent arteriolar resistances [2]. Because NHE3 is a major sodium transport pathway in the renal PT [26], we speculate that the altered levels of apically expressed NHE3 [31] and basolaterally expressed Na^+/K^+-ATPase in the kidney tubules [32] in response to decreased GFR may account for the changes in PT sodium in the cortex of rats given an LP diet. Consistent with this finding, we showed a significant decrease in creatinine clearance in the LP group. We demonstrated that the abundance of NHE3 in the renal cortex was severely decreased after an LP diet. Immunofluorescence analysis confirmed the reduced expression of NHE3 in the apical plasma membrane domains of the proximal convoluted tubule in the kidney cortex of rats given an LP diet. Furthermore, in the LP membrane fractions of the outer stripe of the outer medulla, which include S3 PT segments, we found lower Na^+/K^+-ATPase levels and labeling of Na^+/K^+-ATPase in the basolateral domains of PTs. Moreover, we demonstrated that Na^+/K^+-ATPase activity was reduced in LP isolated microdissected S3 PT segments compared with NP.

These observations support the view that the epithelial transport ability of the PT is impaired in the LP kidney. This condition has been associated with a marked compensatory upregulation of other sodium transporters along the nephron. NKCC-2, which is located in the apical plasma membrane domains of cortical and mTAL segments, mediates apical Na^+-K^+-2Cl co-transport in

these water-impermeable segments [27]. Previous studies show that the abundance of NKCC-2 in TAL is upregulated by 14 days of saline loading, which increases flow and sodium delivery to the thick ascending limb. Conversely, the abundance of NKCC-2 is downregulated by PGE_2 [33].

The increase in NKCC-2 protein levels in the OSOM of the LP group may have resulted in more NaCl being delivered to the loop of Henle. In addition, the low production of PGE_2 in the medulla of rats given the LP diet [34] may have been involved in the upregulation of NKCC-2.

The increased expression of NKCC-2 in the apical membranes of the mTAL may be an important factor in the sodium retention, because the coupled activities of the NKCC-2 and the ROMK channel drive active and passive sodium reabsorption in this portion of the nephron.

Also, K^+ recycling hyperpolarizes the cell membrane potential, which is an essential factor for Cl^- diffusion across the basolateral membrane. Moreover, K^+ recycling across the apical membrane coupled to Cl^- exit across basolateral membranes generates the lumen-positive transepithelial potential that is the main driving force for paracellular Na^+ transport [35]. Patch-clamp studies have demonstrated that the low-conductance K^+ channels (ROMK) contribute to the apical K^+ conductance and to K^+ recycling [12].

We did not find detectable differences in ROMK abundance in the membrane fractions of outer stripe of the outer medulla in the LP group. However, the higher ROMK protein expression in the apical border of the TAL may be linked to ROMK regulation by trafficking and postranslational modification of the channel [36]. Thus, the elevated protein abundance of NKCC-2 and the higher ROMK protein expression demonstrated in the immunofluorescence analysis of the apical membrane of the mTAL of the LP group would be expected to enhance both active and passive NaCl transport [37].

Increased Abundance of NCC, α-, β- and γ-ENaC in Kidney from Rats Given an LP Diet

The thiazide-sensitive NCC is expressed in the DCT, and the amiloride-sensitive ENaC is expressed in the connecting tubule and collecting duct [20]. NCC and the three subunits of ENaC mediate sodium reabsorption, which is regulated by the hormones that control the sodium balance (e.g. the mineralocorticoid aldosterone). Consistent with this, it has recently been suggested that aldosterone stimulates sodium reabsorption by the kidneys, in part, through increasing the abundance of NCC in the DCTs [38] and the α-subunit ENaC in the collecting duct principal cells [19]. In addition, Kim et al. [38] showed an increased NCC abundance in the rat kidney in response to aldosterone infusion and during vasopressin escape. Moreover, the mineralocorticoid antagonist spironolactone decreased the abundance of the NCC protein in the kidney [39]. Although direct mineralocorticoid receptor (MR) regulation of ENaCα gene transcription through its canonical mineralocorticoid response elements (MREs) is important for Na^+ transport activity [40], it is not the only mechanism involved, and serum- and glucocorticoid-regulated kinase (SGK1) might indeed be implicated [41]. Like the gene-encoding ENaCα itself, SGK1 is a classically regulated MR target gene, with MREs driving its expression in response to MRs or glucocorticoid receptors. SGK1 is an immediate early gene that responds rapidly to changes in aldosterone levels by trafficking ENaC to the membrane and potentially single-channel activities [42].

Specifically, in our study, there were marked increases in NCC, α-, β-, and γ-subunits of ENaC. Simultaneously, the increase in these subunits paralleled the higher levels of circulating aldosterone. Upregulation of the ENaC subunits occurred after 14 days of LP feeding. However, we did not study the early aldosterone effects on the collecting duct, including trafficking and postranslational modification of ENaC subunits.

The renin-angiotensin-aldosterone system plays a pivotal role in the pathophysiology of this experimental model of an LP diet [4]. Our results of upregulated NCC and ENaC, previously identified as the major targets of aldosterone-mediated regulation in the kidney [19, 38], indicate that this hormone is involved in regulating distal sodium reabsorption in an LP diet.

Studies of the acute and chronic effects of aldosterone have shown that there is an increase in the turnover rate of the basolateral Na^+/K^+-ATPase and in the insertion of new Na^+/K^+-ATPase units [43]. Na^+/K^+-ATPase provides the pathway for Na^+ exit from the renal tubule epithelial cells in each segment. The transport function is mediated by the α-subunit, whereas the β- and γ-subunits provide regulatory and chaperone functions [44]. After an LP diet, the abundance of the Na^+/K^+-ATPase α_1-subunit did not change. Although mineralocorticoids mediate regulation of Na^+/K^+-ATPase activity in collecting ducts and connecting tubules in an LP diet, possible changes in the abundance of Na^+/K^+-ATPase α_1-subunit protein in these segments may be obscured because, in the majority of the tubular mass (PTs and thick ascending limbs), this sub-

unit is probably not regulated. Na^+/K^+-ATPase activity slightly, but not significantly, increased in microdissected CCD from the LP group.

The levels of the α_1-subunit of Na^+/K^+-ATPase protein expression in the outer stripe of the outer medulla membranes were lower in the LP group than in the NP group. Na^+/K^+-ATPase activity was significantly lower in the isolated microdissected OMCD segment of the LP group than the NP group. Consistent with these findings, we previously reported that an LP diet causes in vivo and in vitro transient dissociation of Na^+/K^+-ATPase from the membrane-cytoskeleton complex in renal outer stripe of the outer medulla (OSOM) [7].

Increased Abundance of ROMK in an LP Diet

The CCD is the site for K^+ secretion and Na^+ reabsorption. The secretory capacity of K^+ diminishes sharply with the transition of the outer medulla [28]. Apical sodium channels permit sodium to passively enter principal cells and to depolarize the apical membrane. The electrical driving force for apical Na^+ entry through ENaC is maintained by K^+ channels [10]. The ROMK renal K^+ channel is the most important channel to serve this function [45].

Consistent with these previous observations, we showed, in addition to a higher protein expression of the three ENaC subunits, a significant increase in the relative protein abundance of ROMK in the renal cortex membrane of the LP group. Moreover, the immunofluorescence study confirmed that the ROMK antibody intensely stained on the apical membrane of principal cells from cortical and medullary collecting duct segments of the LP group. Because we found increased ROMK expression in the apical membranes from collecting duct segments, it is possible that other mechanisms, such as trafficking of transporters to the plasma membrane from intracellular membrane-bound stores with higher surface density of ROMK, could be included in the LP study.

ROMK activity is dependent on direct PKA phosphorylation [46]. All three PKA phospho-acceptor sites in ROMK, embedded within the cytoplasmic NH_2 (Ser-44) and COOH termini (Ser-219 and Ser-313), must be phosphorylated for full channel function. Phosphorylation of the two COOH terminal sites is required to maintain the channel in a high open probability state. Phosphorylation of the NH_2 terminal site, on the other hand, appears to control the number of active channels on the cell surface [47]. Close inspection of the NH_2 terminal PKA site in ROMK reveals that it also falls within a canonical SGK1 phosphorylation sequence [48], suggesting that the channel, and serine 44 in particular, might also be a target of SGK1 [49].

Indeed, the aldosterone-induced kinase SGK1 phosphorylates an N-terminal residue in ROMK, serine 44, which shows a possible molecular mechanism for aldosterone-dependent regulation of the secretory potassium channel in the kidney CCD [50].

We confirmed that the increase in ROMK abundance in response to an LP diet plays a significant role in the higher potassium secretion that contributes to potassium excretion. Aldosterone may be involved in ROMK regulation in an LP diet.

Conclusion

We found that an LP diet is associated with substantial downregulation of NHE3 in the PTs and cTALs of rat kidney and of NKCC-2 in the mTALs, NCC in the DCTs, and ENaC subunits in the connecting segments and collecting ducts. Moreover, we found a marked increase in ROMK1 abundance in CCDs as a result of the LP diet. The increased expression of NCC, α-ENaC subunits, and ROMK1 may increase distal sodium reabsorption and potassium secretion. These factors may explain the hypokalemia resulting from an LP diet because of an increase in fractional potassium excretion. It is likely that increases in NCC, ENaC subunits, and ROMK may be regulated by aldosterone in an LP diet. Readministration of 24% protein in diet recovered protein levels of sodium transporters and potassium channels to control values.

Acknowledgements

This study was financially supported by the National Council of Scientific Research and Technology and from Agencia Nacional de Promoción Científica y Tecnológica (05-12620) to P.G. Vallés.

References

1 Benabe JE, Martinez-Maldonado M: Nutritional influences on renin-angiotensin gene expresion. Nutr Metab Cardiovasc Dis 1996; 6:46–52.
2 Ichikawa I, Pukerson ML, Klahr S, Troy IL, Martinez-Maldonado M, Brenner BM: Mechanism of reduced glomerular filtration rate in chronic malnutrition. J Clin Invest 1980;65:982–988.
3 Kapoor SC, Krishna GG: Protein-induced modulation of renin secretion is mediated by prostaglandins. Am J Physiol 1991;260:688–694.

4 Martinez-Maldonado M, Benabe J, Wilcox J, Wang S, Luo C: Renal renin, angiotensinogen and cANG I-converting-enzyme gene expression: influence of dietary protein. Am J Physiol 1993;264:981–988.
5 Vallés P, Carrizo L, Seltzer A, Manucha W: H^+-ATPase activity in collecting duct segments in protein-deprived rats. Role of angiotensin II on its regulation. Nephron Physiol 2005;99:90–100.
6 Seney FD, Marver D: Protein intake and cation transport in the loop of Henle. J Lab Clin Med 1989;114:587–599.
7 Ruete C, Carrizo L, Vallés P: Na^+/K^+-ATPase stabilization by Hsp70 in the outer stripe of the outer medulla in rats during recovery from low-protein diet. Cell Stress Chaperones 2008;13:157–167.
8 Erinoso HO, Akinbami FO, Akinyinka OO: Prognostic factors in severely malnourished hospitalized Nigerian children. Anthropometric and biochemical factors. Trop Geogr Med 1993;45:290–293.
9 Manary MJ, Brewster DR: Potassium supplementation in kwashiorkor. J Pediatr Gastroenterol Nutr 1997;24:194–201.
10 Giebisch G: Renal potassium transport: mechanisms and regulation. Am J Physiol 1998;274:817–833.
11 Giebisch G, Hebert SC, Wang WH: New aspects of renal potassium transport. Pflügers Arch 2003;446:289–297.
12 Wang W, Hebert SC, Giebisch G: Renal K^+ channels: structure and function. Annu Rev Physiol 1997;59:413–436.
13 Hebert SC: An ATP-regulated, inwardly rectifying potassium channel from rat kidney (ROMK). Kidney Int 1995;48:1010–1016.
14 Palmer LG, Choe H, Frindt G: Is the secretory K channel in the rat CCT ROMK? Am J Physiol 1997;273:404–410.
15 Lu M, Wang T, Yan Q, Yang X, Ke Dong K, Knepper MA, Wang WH, Giebisch G, Shull GE, Hebert SC: Absence of small conductance K+ channel (SK) activity in apical membranes of thick ascending limb and cortical collecting duct in ROMK (Bartter's) knockout mice. J Biol Chem 2002;277:37881–37887.
16 Stokes JB: Potassium secretion by cortical collecting tubule: relation to sodium absorption, luminal sodium concentration, and transepithelial voltage. Am J Physiol 1981; 241:395–402.
17 Brooks HL, Allred AJ, Beutler KT, Coffman TM, Knepper MA: Targeted proteomic profiling of renal sodium transporter and channel abundances in AT1a receptor knockout mice. Hypertension 2002;39:470–473.
18 Masilamani S, Wang X, Kim GH, Brooks H, Nielsen J, Nielsen S, Nakamura K, Stokes JB, Knepper MA: Time course of renal Na-K-ATPase, NHE3, NKCC2, NCC, and ENaC abundance changes with dietary NaCl restriction. Am J Physiol 2002;283:648–657.
19 Masilamani S, Kim GH, Mitchell C, Wade JB, Knepper MA: Aldosterone-mediated regulation of ENaC α, β and γ subunit proteins in rat kidney. J Clin Invest 1999;104: 19–23.
20 Reeves WB, Andreoli TE: Tubular sodium transport; in Schrier RW (ed): Diseases of the Kidney and Urinary Tract. Philadelphia, Lippincott Williams & Wilkins, 2001, pp 135–175.
21 Malnic G, Berliner RW, Giebisch G: Flow dependence of K secretion in cortical distal tubules of the rat. Am J Physiol 1989;256:932–941.
22 Schwartz GJ, Burg MB: Mineralocorticoid effects on cation transport by cortical collecting tubules in vitro. Am J Physiol 1978; 235:576–585.
23 Lombard WE, Kokko JP, Jacobson HR: Bicarbonate transport in cortical and outer medullary collecting tubules. Am J Physiol 1983;244:289–296.
24 Jiang M, Sheetz M: Cargo-activated ATPase activity of kinesin. Biophys J 1985;68:15–16.
25 Preisig PA, Rector FC Jr: Role of Na^+-H^+ antiport in rat proximal tubule NaCl absorption. Am J Physiol 1988;255:461–465.
26 Aronson PS: Role of ion exchangers in mediating NaCl transport in the proximal tubule. Kidney Int 1996;49:1665–1670.
27 Ecelbarger CA, Terris J, Hoyer JR, Nielsen S, Wade JB, Knepper MA: Localization and regulation of the rat renal Na-K-2Cl cotransporter, BSC-1. Am J Physiol Renal Fluid Electrolyte Physiol 1996;271:619–628.
28 Muto S: Potassium transport in the mammalian collecting duct. Physiol Rev 2001;81:85–116.
29 Kohda Y, Ding W, Phan E, Housini I, Wang J, Star RA, Huang CL: Localization of the ROMK potassium channel to the apical membrane of distal nephron in rat kidney. Kidney Int 1998;54:1214–1223.
30 Tumlin JA, Hoban CA, Medford RM, Sands JM: Expression of Na-K-ATPase α- and β-subunit mRNA and protein isoforms in the rat nephron. Am J Physiol 1994;266:240–245.
31 Amemiya M, Loffing J, Lotscher M, Kaissling B, Alpern RJ, Moe OW: Expression of NHE-3 in the apical membrane of rat renal proximal tubule and thick ascending limb. Kidney Int 1995;48:1206–1215.
32 Jorgensen PL: Sodium and potassium ion pump in kidney tubules. Physiol Rev 1980; 60:864–917.
33 Fernandez-Llama P, Ecelbarger CA, Ware JA, Andrews P, Lee AJ, Turner R, Nielsen S, Knepper MA: Cyclooxygenase inhibitors increase Na-K-2Cl cotransporter abundance in thick ascending limb of Henle's loop. Am J Physiol 1999;277:219–226.
34 Yanagisawa H, Wada O: Effects of dietary protein on eicosanoid production in rat renal tubules. Nephron 1998;78:179–186.
35 Hebert S, Desir G, Giebisch G, Wang W: Molecular diversity and regulation of renal potassium channels. Physiol Rev 2000;85:319–371.
36 O'Connell AD, Leng Q, Dong K, MacGregor GG, Giebisch G, Hebert SC: Phosphorylation-regulated endoplasmic reticulum retention signal in the renal outer-medullary K^+ channel (ROMK). Proc Natl Acad Sci 2005;102:9954–9959.
37 Hoagland KM, Flasch AK, Dahly Vernon AJ, dos Santos EA, Knepper MA, Roman RJ: Elevated BSC-1 and ROMK expression in Dahl salt-sensitive rat kidneys. Hypertension 2004;43:860–865.
38 Kim GH, Masilamani S, Turner R, Mitchell C, Wade JB, Knepper MA: The thiazide-sensitive Na-Cl cotransporter is an aldosterone-induced protein. Proc Natl Acad Sci USA 1998;95:14552–14557.
39 Abdallah JG, Schrier RW, Edelstein C, Jennings SD, Wyse B, Ellison DH: Loop diuretic infusion increases thiazide-sensitive Na^+/Cl^--cotransporter abundance: role of aldosterone. J Am Soc Nephrol 2001;12:1335–1341.
40 May A, Puoti A, Gaeggeler HP, Horisberger JD, Rossier BC: Early effect of aldosterone on the rate of synthesis of the epithelial sodium channel alpha subunit in A6 renal cells. J Am Soc Nephrol 1997;8:1813–1822.
41 Boyd C, Naray-Fejes-Toth A: Gene regulation of ENaC subunits by serum- and glucocorticoid-inducible kinase-1. Am J Physiol Renal Physiol 2005;288:F505–F512.
42 Pearce D, Kleyman TR: Salt, sodium channels, and SGK1. J Clin Invest 2007;117:592–595.
43 Sansom SC, O'Neil RG: Effects of mineralocorticoids on transport properties of cortical collecting duct basolateral membrane. Am J Physiol 1986;251:743–757.
44 McDonough AA, Farley RA: Regulation of Na,K-ATPase activity. Curr Opin Nephrol Hypertens 1993;2:725–734.
45 Wang W: Renal potassium channels: recent developments. Curr Opin Nephrol Hypertens 2004;13:549–555.
46 McNicholas CM, Wang W, Ho K, Hebert SC, Giebisch G: Regulation of ROMK1 K+ channel activity involves phosphorylation processes. Proc Natl Acad Sci USA 1994;91: 8077–8081.
47 MacGregor GG, Xu JZ, McNicholas CM, Giebisch G, Hebert SC: Partially active channels produced by PKA site mutation of the cloned renal K+ channel, ROMK2 (kir1.2). Am J Physiol 1998;275:F415–F422.
48 Kobayashi T, Cohen P: Activation of serum- and glucocorticoid-regulated protein kinase by agonists that activate phosphatidylinositide 3-kinase is mediated by 3-phosphoinositide-dependent protein kinase-1 (PDK1) and PDK2. Biochem J 1999;339:319–328.
49 Lin HD, Sterling H, Wang WH: The protein tyrosine kinase-dependent pathway mediates the effect of K intake on renal K secretion. Physiology 2005;20:140–146.
50 Kim BY, Campo C, Nance L, King A, Maouyo D, Welling PA: Cell surface expression of the ROMK (Kir 1.1) channel is regulated by the aldosterone-induced kinase, SGK-1, and protein kinase A. J Biol Chem 2003;278: 23066–23075.